CEBAF Program Advisory Committee Six (PAC6) Proposal Cover Sheet

This proposal must be received by close of business on April 5, 1993 at:

CEBAF
User Liaison Office
12000 Jefferson Avenue
Newport News, VA 23606

Proposal Title

TWO PION DECAY OF ELECTRO PRODUCED BARYON RESONANCES

Contact Person

Name: MARCO RIPANI
Institution: INFN - GRUPPO 3
Address: VIA DODECANNESO 33
Address:
City, State ZIP/Country: GENOVA I-16146 ITALY
Phone: 0113 9-10-353645 8 **FAX:** 0113 9-10-313358
E-Mail → BITnet: RIPANI@VAXGE.INFN.IT **Internet:**

If this proposal is based on a previously submitted proposal or letter-of-intent, give the number, title and date:

CEBAF Use Only

Receipt Date: 4/2/93 Log Number Assigned: PR 93-006

By: gp

TWO PION DECAY OF ELECTROPRODUCED LIGHT QUARK BARYON RESONANCES

The N^* Group in the CLAS Collaboration

Spokespersons: M. Ripani and V. Burkert

W. Brooks, V. Burkert, B. Mecking, B. Niczyporuk, E. Smith, A. Yegneswaran
CEBAF, Newport News, Virginia

D. Crabb, D. Day, R. Marshall, J. McCarthy, R. Minehart, D. Pocanic
O. Rondon-Aramayo, R. Sealock, L.C. Smith, S. Thornton, H.J. Weber
University of Virginia, Charlottesville, Virginia

G. Adams, N. Mukhopadyay, P. Stoler
Rensselaer Polytechnic Institute, Troy, New York

C. Carlson, A. Coleman, H. Funsten, T. Tung
College of William and Mary, Williamsburg, Virginia

D. Doughty, D. Heddle, Zh. Li
Christopher Newport University, Newport News, Virginia

R. Chasteler, D.R. Tilley, H. Weller
Duke University, Durham, North Carolina

N. Bianchi, G.P. Capitani, E. De Sanctis, P. Levi Sandri, V. Muccifora
E. Polli, A.R. Reolon, P. Rossi
Instituto Nazionali di Fisica Nucleare, Frascati, Italy

M. Anghinolfi, P. Corvisiero, G. Gervino, L. Mazzaschi, V.I. Mokeev,
G. Ricco, M. Ripani, M. Sanzone, M. Taiuti, A. Zucchiatti
Instituto Nazionali di Fisica Nucleare, Genova, Italy

D. Isenhower, M. Sadler
Abilene Christian University, Abilene, Texas

L. Dennis, P. Dragovitsch
Florida State University, Tallahassee, Florida

K. Beard
Hampton University, Hampton, Virginia

S. Dytman
University of Pittsburgh, Pittsburgh, Pennsylvania

K. Giovanetti
James Madison University, Harrisonburg, Virginia

M. Manley
Kent State University, Kent, Ohio

J. Lieb
George Mason University, Fairfax, Virginia

M. Gai
Yale University, New Haven, Connecticut

Abstract

The two pion electroproduction process on the nucleon ($eN \rightarrow e'N\pi\pi$) will be used in the mass region between threshold and 2.2 GeV both to investigate poorly known baryon resonances and to search for "missing" states that are predicted by quark models but have not yet been found experimentally. The electron beam allows to vary both the energy and momentum transfer exploring the Q^2 dependence of the couplings. Many of these baryon resonances should have a large branching ratio in the $\Delta\pi$ and in the $N\rho$ channel, both giving a finale state with $N\pi\pi$. Using the CEBAF Large Acceptance Spectrometer CLAS, the hadronic products will be detected in coincidence with the scattered electron. This makes it possible to measure the differential cross section for the production of $\Delta\pi$ and ρN and the decay angular distribution of the Δ and the ρ, which are both especially sensitive to resonance contributions.

A. Scientific Motivation

Understanding the structure of baryons in terms of the fundamental interaction of the constituent quarks and gluons is one of the challenges in strong interaction physics. This interaction is governed by QCD. However, solutions of this theory in the non-perturbative domain of the interaction are extremely difficult to achieve. The lattice gauge approach offers the best hope for exact calculations, but results seem to be far in the future. Thus, models will continue to play an important role. Microscopic models that utilize ingredients from QCD relate the internal structure of baryons to the strong interaction of the confined constituents in an "effective" description. Probing the baryons structure with electromagnetic probes at distance scales of 0.5 fermi or less, will give us detailed insight into this interaction.

The excitation of baryons resonances at low momentum transfer is genuinely a non-perturbative phenomenon. Measurements of the transition amplitudes from the ground state nucleon to excited states are sensitive to the internal spatial structure of the excited state, as well as to the spin structure of the transition. Resonance transitions to states in the lower mass region $M < 1.7GeV$ can be studied effectively using the single pion or eta decay channels. Nearly all of our knowledge about the electromagnetic coupling of light quark baryons comes from photo- or electroproduction of these channels. Several proposals by the N^* group to vastly improve information about these channels have already been approved[17].

In the mass region region above $\sim 1.7GeV$ the single pion and eta channels become less effective in the study of resonance excitations as many states tend to decouple from these channels. Measurement of states such as $S_{31}(1650)$, $D_{13}(1700)$, and $D_{33}(1700)$ have been very difficult in the single-pion channel due to the small branching ratio into this channel. However, information about the electromagnetic transition formfactors of these states is crucial for testing symmetry properties underlying the light-quark baryons structure. For example, it will allow testing the assumption that resonance excitations proceed through a single quark transition [1]. From πN scattering experiments we know that many of the higher mass states decay dominantly in multi-pion channels, such as $\Delta\pi$ or $N\rho$, leading to $N\pi\pi$ final states (see Table 1). Exploration of some of these states in electroproduction is one of the two main objectives of this proposal.

Table 1: N* resonances with B(N* $\rightarrow$ more than one pion) > 30%

Res.	Mass (MeV)	Γ (MeV)	B ($N\pi\pi$) (%)	B($\Delta\pi$) (%)	B(Nρ) (%)	B(p.s.) (%)
$P_{11}\ \frac{1}{2}^+$	1400 - 1480	120 - 350	30 - 50	10 - 20	10 - 15	5-20
$D_{13}\ \frac{3}{2}^-$	1510 - 1530	100 - 140	40 - 50	20 - 30	15 - 25	< 5
$S_{31}\ \frac{1}{2}^-$	1600 - 1650	120 - 160	65 - 75	60 - 70	10 - 20	-
$D_{15}\ \frac{5}{2}^-$	1660 - 1690	120 - 180	60 - 65	55 - 60	< 10	< 5
$F_{15}\ \frac{5}{2}^+$	1670 - 1690	110 - 140	35 - 45	10 - 15	10 - 20	15 - 20
$D_{13}\ \frac{3}{2}^-$	1670 - 1730	70 - 120	80 - 90	15 - 70	< 20	< 70
$D_{33}\ \frac{3}{2}^-$	1630 - 1740	190 - 300	80 - 90	50 - 90	< 35	< 40

The SU(6) symmetric quarkmodel[2,3] predicts many more states than have been found in well studied channels such as $\pi N \rightarrow \pi N$. In the QCD improved version of this model, this fact is explained by QCD mixing effects leading to the decoupling of many of these states from the single pion channel. Consequently, they are not expected to be seen in elastic πN scattering experiments. However, other models such as the quark cluster model[18] have been developed, which, due to a reduced number of internal degrees of freedom, predict a fewer number of states than the symmetric model in accordance with the experimental observation. Clearly, existence or non-existence of these states will be a crucial test

of the symmetry properties underlying the light quark baryon spectroscopy. If these states did not exist, our current picture of light quark baryon structure could change dramatically. Search for at least some of these states is called for and is crucial in discriminating between alternate approaches for modeling the baryon structure. Search for some of the "missing" states (see Table 2) is the second main objective of this proposal.

Table 2: Resonances predicted by quark models which are not coupled to the πN channel, but which are predicted to couple strongly to the $\pi\pi$N channel (from Ref. 3)

State	Mass (MeV)	Multiplet	Decay
F_{15}	1955	$(70,2^+)$	ωN, $\Delta\pi$, ρ N
F_{15}	2025	$(70,2^+)$	ωN, $\Delta\pi$
P_{13}	1955	$(70,2^+)$	$\Delta\pi$ (P-wave)
P_{13}	1980	$(70,2^+)$	$\Delta\pi$ (F-wave)
P_{31}	1875	$(56,2^+)$	ρ N
F_{35}	1975	$(70,2^+)$	$\Delta\pi$, ρ N

How can we search for these states? The QCD improved quarkmodel predicts many of these states to couple strongly to the two-pion channel through decays such as $N^* \rightarrow \Delta\pi$ or $N^* \rightarrow N\rho$. Our study therefore focuses on isolating these channels.

In the total photoabsorption cross section on the proton above 400 MeV photon LAB energy two pion production becomes possible, as shown clearly by several data from bubble chamber experiments[4]. The total photoabsorption cross section and contributions from various multi-pion channels are shown in Figure 1; the dominance of multi-pion processes for W > 1.6 GeV is clearly visible. In this proposal we concentrate on the process

$$eN \rightarrow e'N'\pi\pi$$

on protons and neutrons, showing that it will be possible to extract information on poorly known and "missing" baryon resonances. Exploiting the Q^2 degree of freedom in electroproduction is an important aspect in this study since many of the "missing" resonances are states of highly excited 3-quark orbital angular momentum whose photocoupling amplitudes are predicted to become more important at higher Q^2.

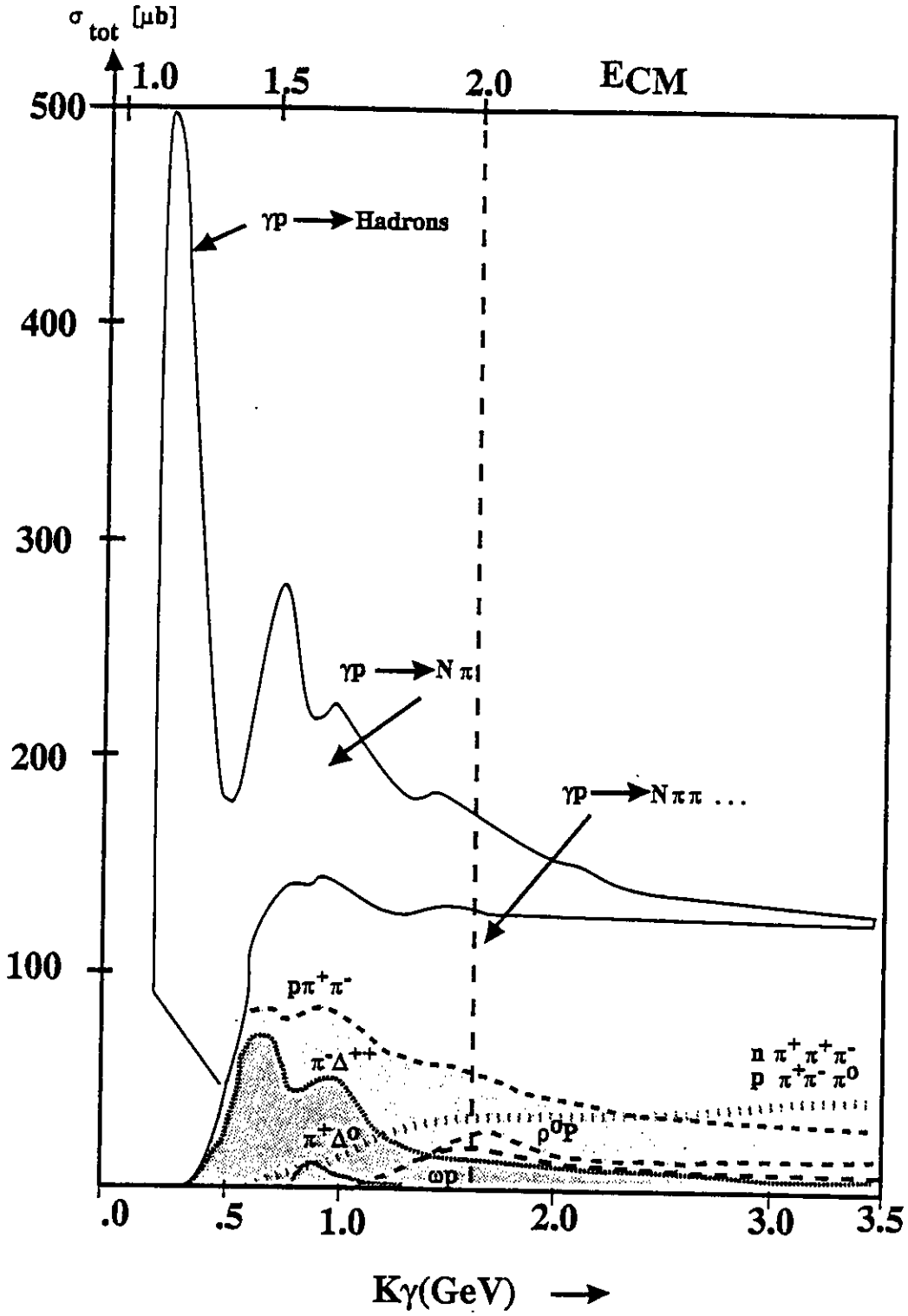

Figure 1: *Total photoabsorption cross section on protons. Also shown is the approximate breakdown into exclusive channels.*

Main contributing channels to this process are:

a. $\Delta(1236)$ production: $eN \rightarrow e'\Delta\pi \rightarrow e'(N\pi)\pi$

b. ρ meson production: $eN \rightarrow e'N\rho \rightarrow e'N(\pi\pi)$

(where the brackets indicate that a peak in the invariant mass of the pair should be expected)

There is also a phase space contribution

c. $eN \rightarrow e'N\pi\pi$

All these reactions can proceed through continuum processes, described at low energies by Born terms, or through the excitation of baryon resonances. Separation of the resonance contribution to a particular reaction channel allows to study the higher resonances without the contamination of the $\Delta(1236)$ which contributes to one-pion production only.

B. Existing Data

The two-pion-production data come mainly from bubble chamber experiments with real photons[1]. Of the three possible double pion production processes on protons

$$\gamma p \rightarrow p\pi^+\pi^-$$
$$\gamma p \rightarrow p\pi^o\pi^o$$
$$\gamma p \rightarrow n\pi^+\pi^o$$

only the first one has been studied, the other two are not observable in bubble chamber experiments; of the charge symmetric reactions

$$\gamma n \rightarrow n\pi^+\pi^-$$
$$\gamma n \rightarrow n\pi^o\pi^o$$
$$\gamma n \rightarrow p\pi^-\pi^o$$

only the second one was not observable, while cross sections for the other two have been deduced from photoproduction experiments on deuterium. The total photoproduction cross section of charged pion pairs $\pi^+\pi^-$ on protons is shown in Figure 2.

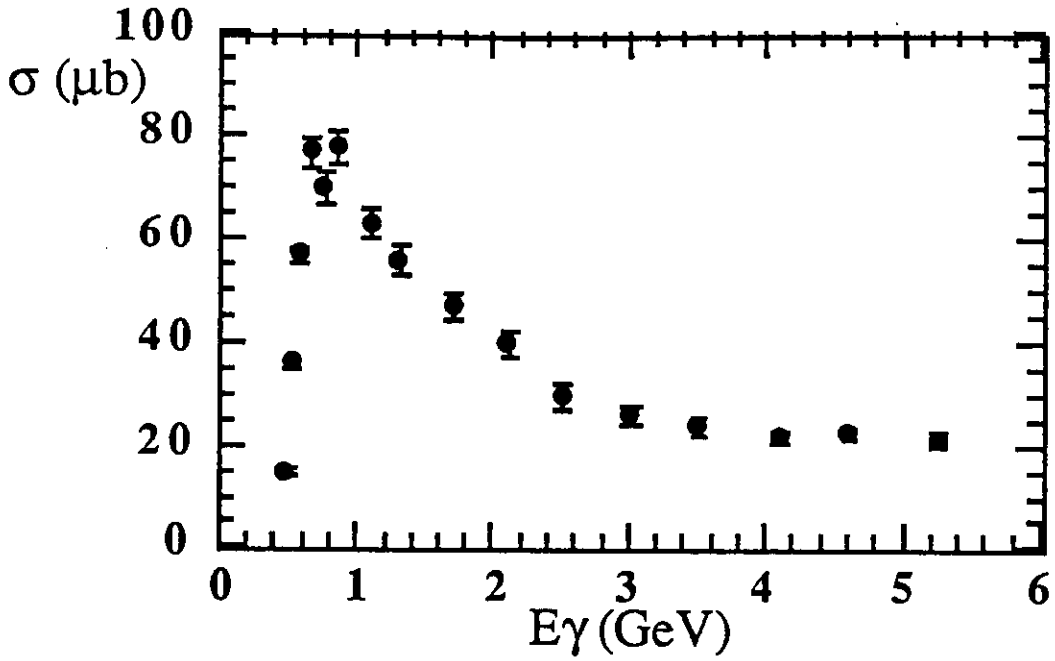

Figure 2: *Total cross section for the reaction $\gamma p \rightarrow p\pi^+\pi^-$ as a function of the photon laboratory energy E_γ. Data from ref. 4*

In the analysis of bubble chamber data, the different contributing processes have been separated using combined fits in the invariant masses of the hadronic pairs; the main results are that the $p\pi^+\pi^-$ channel is dominated by strong $\Delta^{++}\pi^-$ production for photon LAB energies between 400 and about 1 GeV (corresponding to W between 1.4 and 1.7 GeV) with a cross section that steeply rises above threshold and then decreases smoothly with increasing photon energy, while above 1 GeV ρ^o production becomes the main process with a cross section nearly independent of energy within a few GeV. The CMS angular distribution of the π^- produced together with the Δ^{++} turns out to be nearly isotropic near the threshold, while becoming more forward-peaked as the energy increases. The angular distribution of the ρ^o shows at the contrary a diffraction-like behavior being strongly forward-peaked.

Only a few data points exist for two pion electroproduction, with W around 1.4 GeV, and some low statistics measurements at higher masses[6]. However, no attempt was made to search for resonance structure.

C. Cross Section Calculations

Model calculations have been carried out to determine the sensitivity of the two pion production channel to the presence of resonances. Figure 3 shows the Feynman diagrams describing the processes involved in $\Delta\pi$ photoproduction[7,8]. The production of a Δ together with a charged pion is dominated by the first two diagrams, that is the "contact" interaction and the "pion-in-flight" process, while these diagrams are absent in the case of production of a neutral pion. The resonant part of the hadronic current is constructed using the photocouplings $S_{\frac{1}{2}}$, $A_{\frac{1}{2}}$, $A_{\frac{3}{2}}$ and an effective decay interaction[6,7].

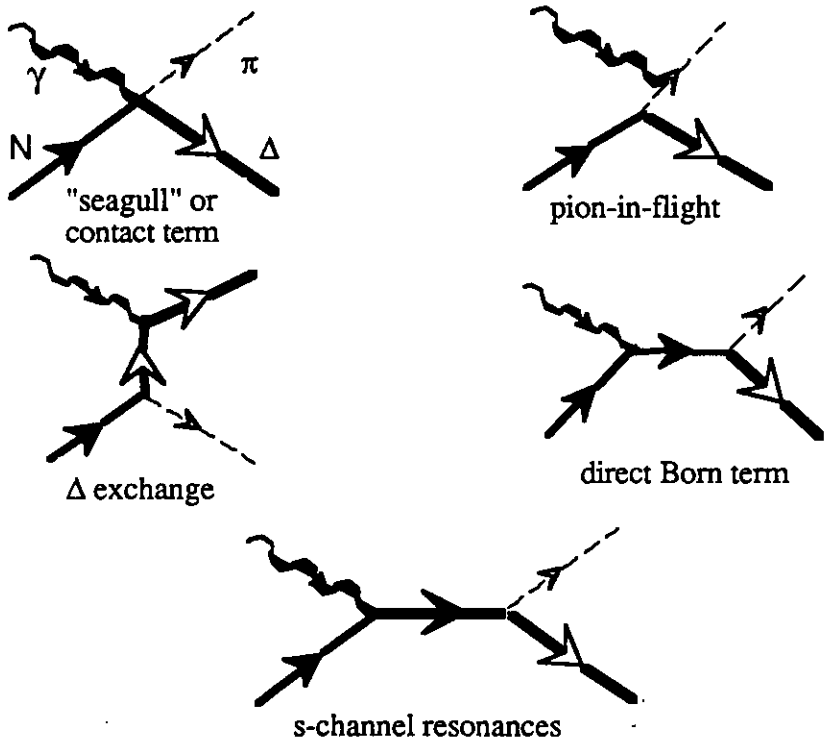

Figure 3: *Processes contributing to $\Delta\pi$ production off the nucleon*[7]

Figure 4 depicts the processes involved in ρ meson production[11]. The diffraction scattering is important at low values of the invariant momentum transfer t, that is at forward CMS angles of ρ production[4,12]; the pion-in-flight term also has a differential cross section decreasing with t. The resonant contributions are constructed in the same way as in the $\Delta\pi$ production.

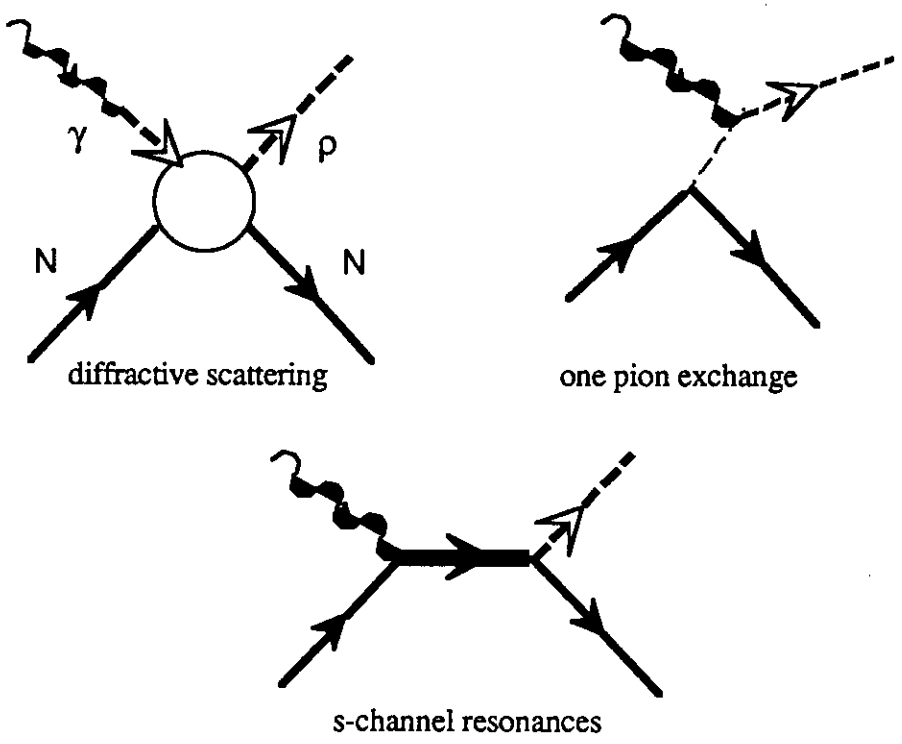

Figure 4: *Feynman diagrams for processes contributing to ρN production*[11]

Concerning the Q^2 dependence of the Born terms for the $\Delta\pi$ case, some data show evidence for a Vector Meson Dominance behavior of the $\Delta^{++}\pi^-$ electroproduction at threshold[6]; assuming this as a guideline, the Born amplitudes for the $\Delta\pi$ process have been multiplied by a dipole-like form factor with the ρ mass as parameter. Employing the Vector Meson Dominance Model for the ρN process, the Born amplitudes have been multiplied by a ρ propagator. Concerning the Q^2 dependence of the photocouplings of the resonances that have been measured[9], a reasonable compromise between quark model calculations and data has been used as deduced from Ref. 13. For the case of "missing" resonances, quark model predictions by Koniuk and Isgur[2] were used for the photocoupling amplitudes. A prescription by Foster and Hughes[14] was employed to establish the Q^2 evolution of the amplitudes.

To check the calculation, $\Delta^{++}\pi^-$ production and ρ^op production in the limit of real photons is considered introducing the Born terms and two well known resonances, that is the $D_{13}(1520)$ and the $F_{15}(1688)$.

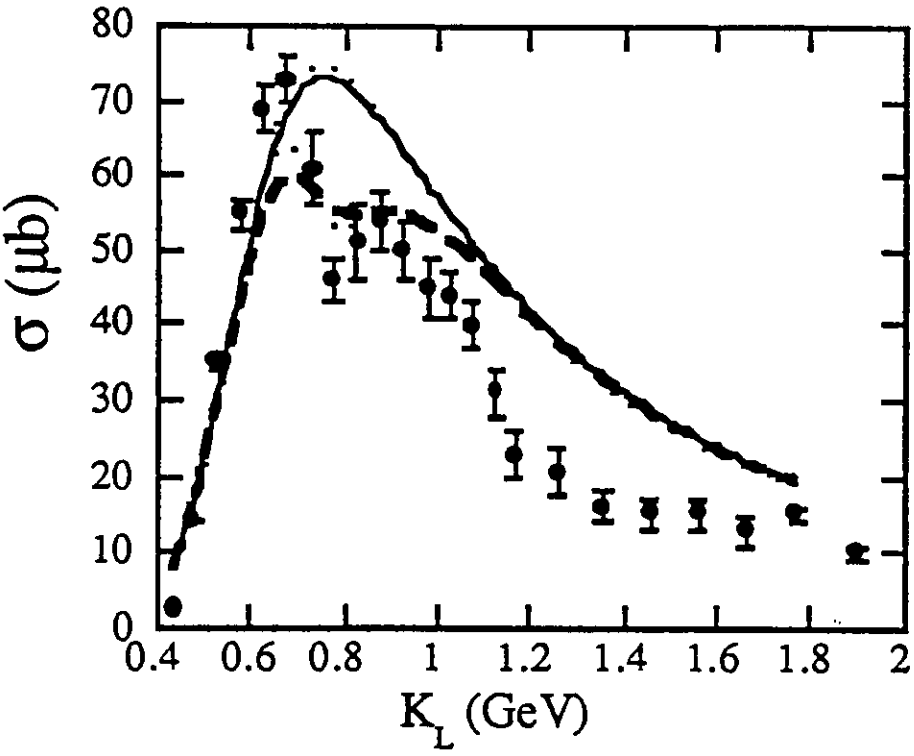

Figure 5: *Cross section for $\Delta^{++}\pi^-$ photoproduction versus the LAB photon energy. Full curve: this calculation, including the two dominant Born terms; dashed curve: this calculation, including the Born terms and the $D_{13}(1520)$ and the $F_{15}(1688)$ resonances; data points are from Ref.4.*

Figure 5 shows the calculated total cross section for the $\pi^-\Delta^{++}$ process as a function of the LAB photon energy K_L together with the data from ref. 4. In Figure 6 the differential cross section for $\Delta^{++}\pi^-$ photoproduction is compared with the same data. The agreement is sufficiently good that we are confident that the calculation may be applied at other kinematics as well.

Figure 7 shows the total cross section for the ρ^0p channel as a function of the photon LAB energy, while Figure 8 shows the differential cross section for the same channel as a function of the invariant momentum transfer t: The resonant contributions can be clearly seen in the angular distributions at large t, or backward CMS angles.

The decay angular distribution of the produced Δ or ρ will give further information about the contributing processes[4].

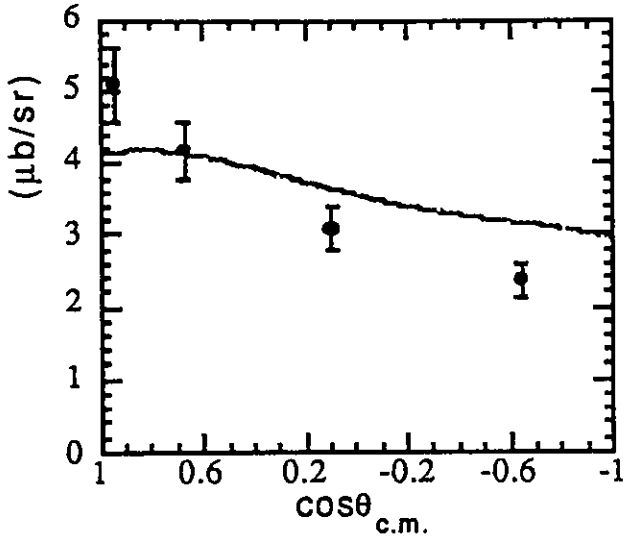

Figure 6: *Differential cross section for $\Delta^{++}\pi^-$ photoproduction as a function of the CMS pion angle at $W = 1.4$ GeV. Full curve: this calculation, including the two dominant Born Terms, the $D_{13}(1520)$ and the $F_{15}(1688)$ resonances; data points are from Ref. 4.*

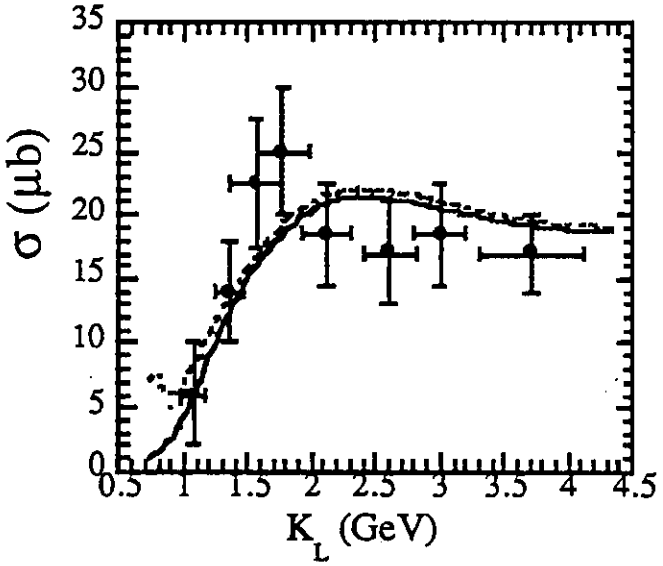

Figure 7: *Cross section for $\rho^0 N$ photoproduction as a function of the LAB photon energy K_L. Full curve: this calculation, including the Born terms; dashed curve: this calculation, including the Born terms plus the $D_{13}(1520)$ and the $F_{15}(1688)$ resonances; data points are from Ref. 4.*

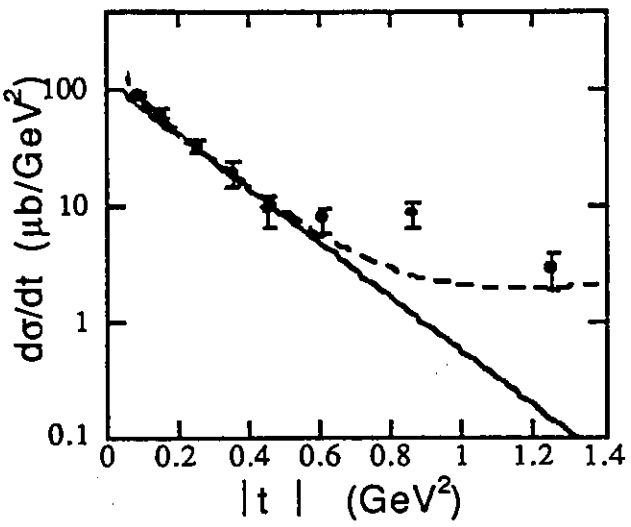

Figure 8: *Differential cross section for ρ^0 photoproduction on protons versus the invariant momentum transfer t, at $W = 2GeV$. Solid Curve: This calculation, including the diffractive process and the OPE; dashed curve: diffractive process + OPE + $D_{13}(1520)$ + $F_{15}(1688)$; data points are from Ref. 4.*

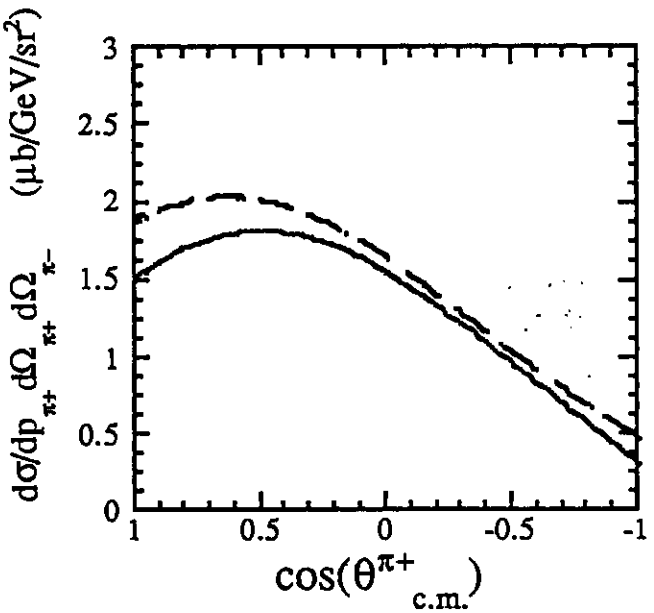

Figure 9: *Differential cross section for the process $\gamma p \to \Delta^{++}\pi^- \to p\pi^+\pi^-$ at $\theta_{cm}(\pi^-) = 0^0$; $W = 1.44$ GeV; $Q^2 = 0$.*

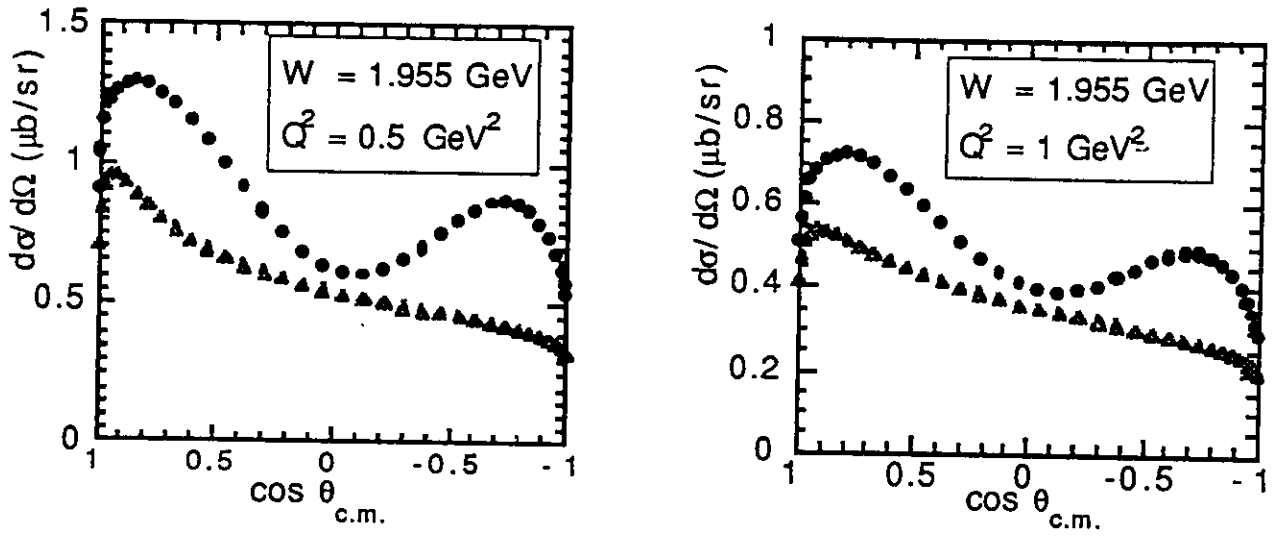

Figure 10: *Differential cross section for $\Delta^{++}\pi^-$ photoproduction versus the pion CMS angle. Triangles: Born terms, without resonances; solid curve: Born terms + $F_{15}(1955)$*

Using the calculation for the $\Delta^{++}\pi^-$ channel and introducing the operator for the Δ decay, the angular correlation of the second pion (the π^+ coming from the Δ decay) and its sensitivity to the presence of resonances have been studied. For this evaluation a spin 1/2 resonance, the $P_{11}(1440)$ has been introduced. In this case the total angular momentum J of the process is different from the main "contact" graph background, which corresponds to J = 3/2. This should result in a different population of the helicity states of the produced Δ and therefore in a different decay angular distribution of the Δ itself. Figure 9 shows the differential cross section for the final state $p\pi^+\pi^-$ as a function of the π^+ CMS angle for a fixed configuration of Δ^{++} production. The quantity is indeed sensitive to the presence of the resonant state. Differences in the population of helicity states can also be expected for higher resonant states and is another tool for disentangling resonances and nonresonant contributions.

In a second step, a "missing" resonance was introduced in the calculation to study the sensitivity for this case. As a candidate, the $F_{15}(1955)$ was chosen, having both a strong photocoupling and a strong decay coupling in the $\Delta\pi$ and the ρN channels, as predicted by quark models. In Figures 10 - 13 the results of the calculations are shown for the differential cross sections of various channels and for two values of Q^2. Figure 14 shows the predicted cross section ratio of $F_{15}(1955)$ resonance excitation and the nonresonant Born term contributions. The resonant contribution becomes relatively more important with increasing Q^2.

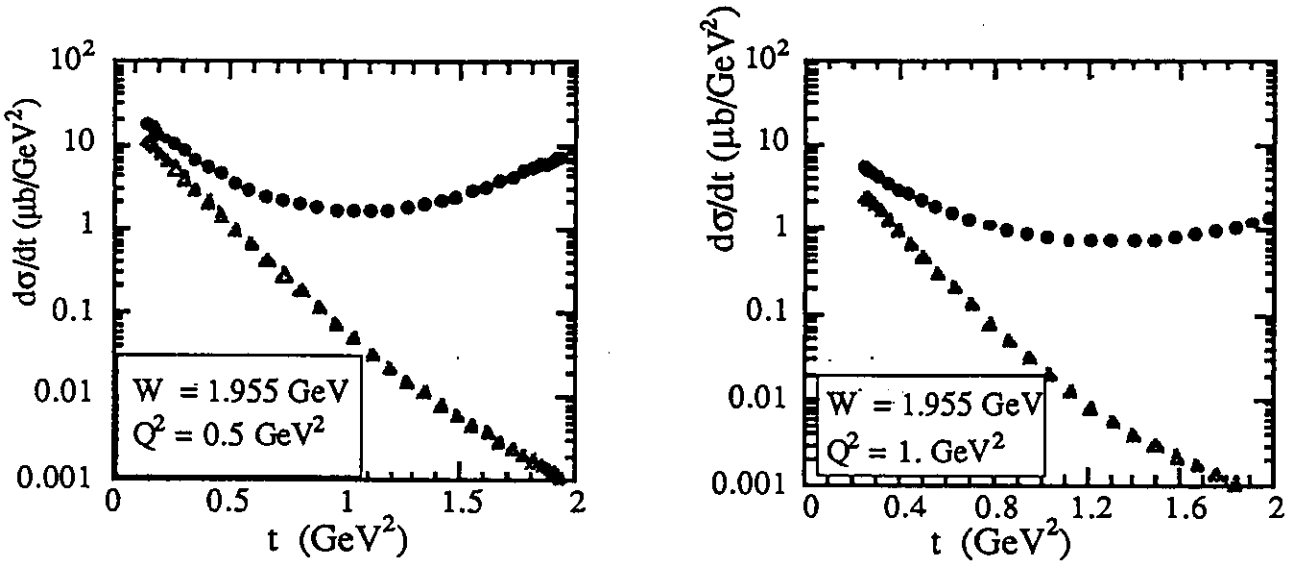

Figure 11: *Differential cross section for ρ^0 photoproduction as a function of the CMS ρ^0 angle. Triangles: Born terms, without resonances; full circles: Born terms + $F_{15}(1955)$ resonance.*

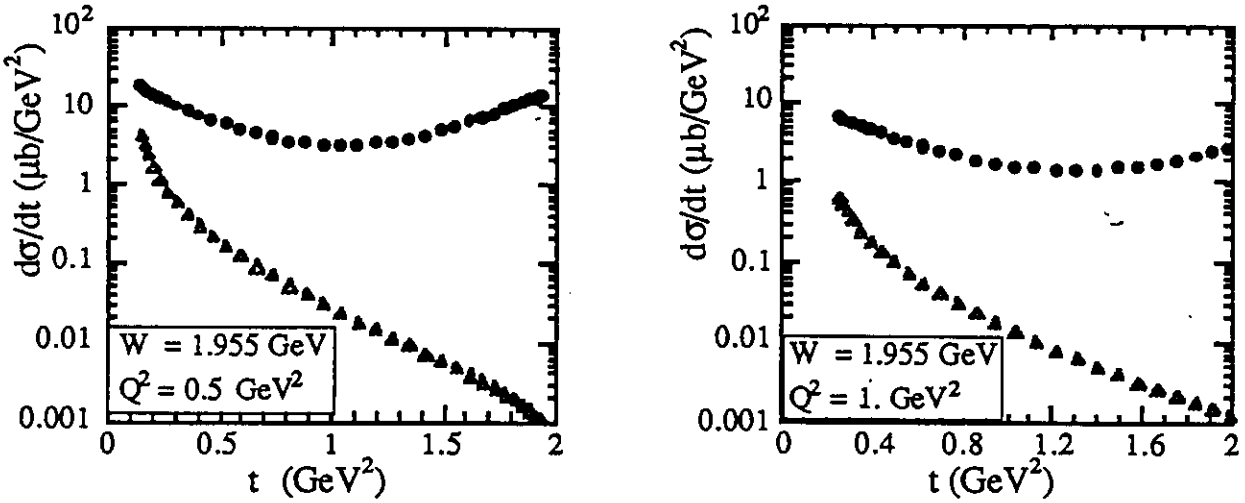

Figure 12: *Differential cross section for ρ^+ photoproduction versus the CMS ρ^+ angle. Triangle: Born terms, without resonances; full circles: Born terms + $F_{15}(1955)$ resonance.*

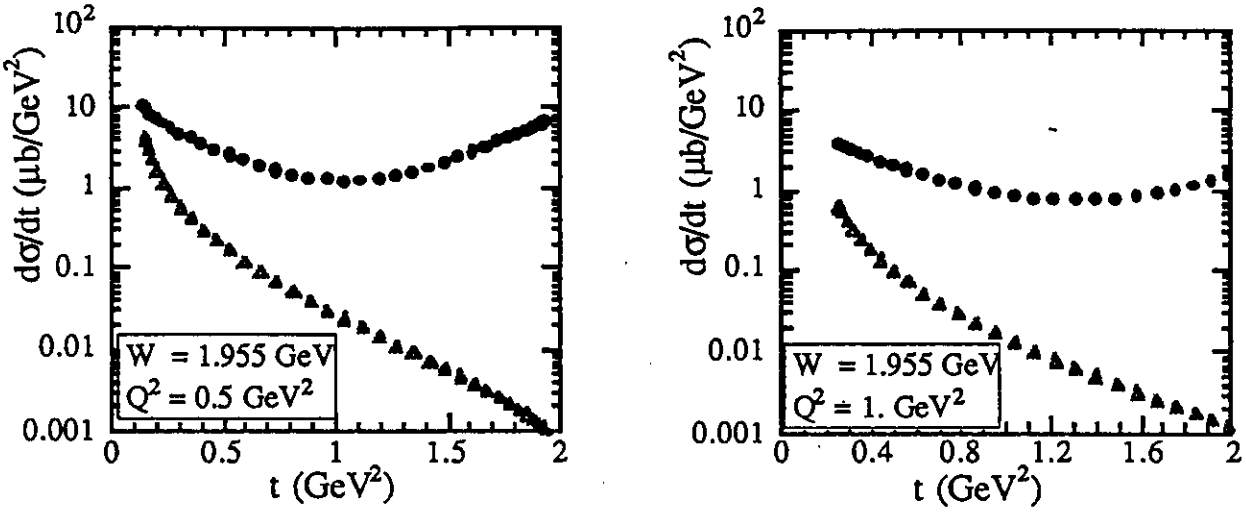

Figure 13: *Differential cross section for ρ^- photoproduction on neutrons versus the ρ^- CMS angle. Triangle: Born terms, without resonances; circles: Born terms + $F_{15}(1955)$ resonance.*

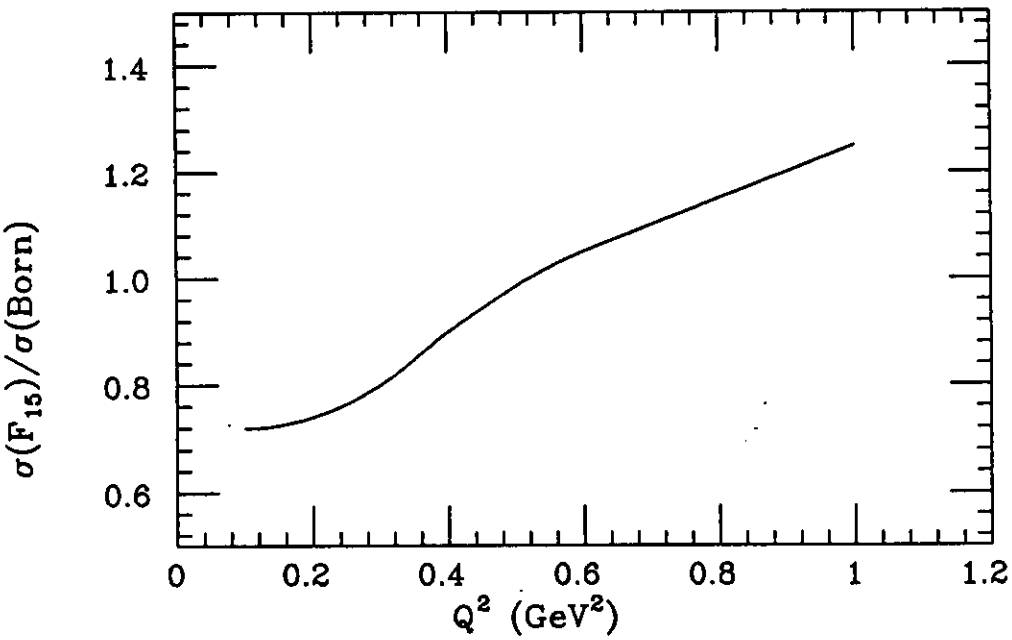

Figure 14: *Ratio of total cross sections for $\Delta^{++}\pi^-$ production from the $F_{15}(1955)$ resonance and from the nonresonant Born contributions.*

Two observations are worth noting:

1) Very interesting channels are those containing a neutral pion or a charged ρ meson, like $\Delta^+\pi^o$ and ρ^+n on proton, because in these cases the Born term contribution is considerably reduced or almost absent.

2) Increasing Q^2 helps separating the resonant contribution from the Born continuum.

The following table compiles the proposed channels to be measured and the physics that may be extracted:

measurement	**channels**	**physics information**
ep$\rightarrow$ep$\pi^+\pi^-$	$\Delta^{++}\pi^-$ and ρ^o production	$\Delta^{++}\pi^-$ has a high Born background but decreasing with energy; moreover, angular dependence of the $\Delta\pi$ cross section gives information about the resonant partial waves
ep$\rightarrow$en$\pi^+\pi^o$	$\Delta^+\pi^o$ and ρ^+ production	$\Delta^+\pi^o$ has a negligible Born background; therefore it is very sensitive to resonance contributions, similar situation for ρ^+ because of the absence of the strong diffractive production
en$\rightarrow$ ep$\pi^-\pi^o$	$\Delta^o\pi^o$ and ρ^- production	$\Delta^0\pi^o$ has a negligible Born background; therefore it is very sensitive to resonance contributions, similar situation for ρ^- because of the absence of the strong diffractive production

D. Experimental Method

The proposed experiment will use the CEBAF Large Acceptance Spectrometer to measure $\Delta\pi$ and ρN electroproduction off protons and neutrons. The goal of the experiment is to measure total and differential cross sections for these channels as a function of the mass of the hadronic system W, of Q^2 and of the production angles. Differential cross sections will be measured by detecting the hadronic products in coincidence with the scattered electron, and using invariant mass analysis to separate the $\Delta\pi$ and ρN contributions. A subset of data will contain information about the decay correlation of Δ and ρ, allowing to get additional sensitivity to resonance formation.

Resonant and nonresonant contributions will be separated by employing well established partial wave analysis techniques. Both the angular and energy dependence of the $\gamma_v p \rightarrow \Delta\pi$ and the $\gamma_v p \rightarrow N\rho$ differential cross sections will be analysed. In this analysis, constraints from other channels such as the $N\pi$, $p\eta$, and $p\omega$ will be used as well.

E. Simulation of the Experiment

An event generator[15] has been developed which includes contribution of all relevant channels (one, two, three, $\cdots$ pion production), to simulate the experimental situation and to study the response of the CLAS detector (acceptance, resolution, mass separation). The generated events have been traced through the CLAS standard simulation packages (FASTMC and SDA). Figure 15 shows a single $e^- p \rightarrow e^- p\pi^+\pi-$ events for a 4GeV beam energy, and a hadronic mass of W = 1.7GeV. Figure 16 shows the missing mass reconstruction in the CLAS when measuring $p\pi^+\pi^-$ in coincidence with the electron. Owing to the good momentum and angular resolution of CLAS, one, two and three pion production processes can be well separated. At full magnetic field the overall efficiency for detecting the three charged hadrons is about 11%, while at half magnetic field it is about 15%. The overall efficiency is significantly increased if the data are included where only two hadrons are detected, and missing mass techniques are used to reconstruct the not detected third hadron.

Figure 17 and 18 show the reconstruction of the $p\pi^+$ and the $\pi^+\pi^-$ invariant masses, showing clearly the Δ^{++} and ρ^o peaks in the invariant mass distribution.

Simulations have been carried out also for the detection of neutrals. This will allow measurement of channels which are of particular interest as they are little affected by Born background. In this case efficiencies are lower due to the fact that neutrons and photons are detected only in the shower calorimeter, with reduced solid angle acceptance.

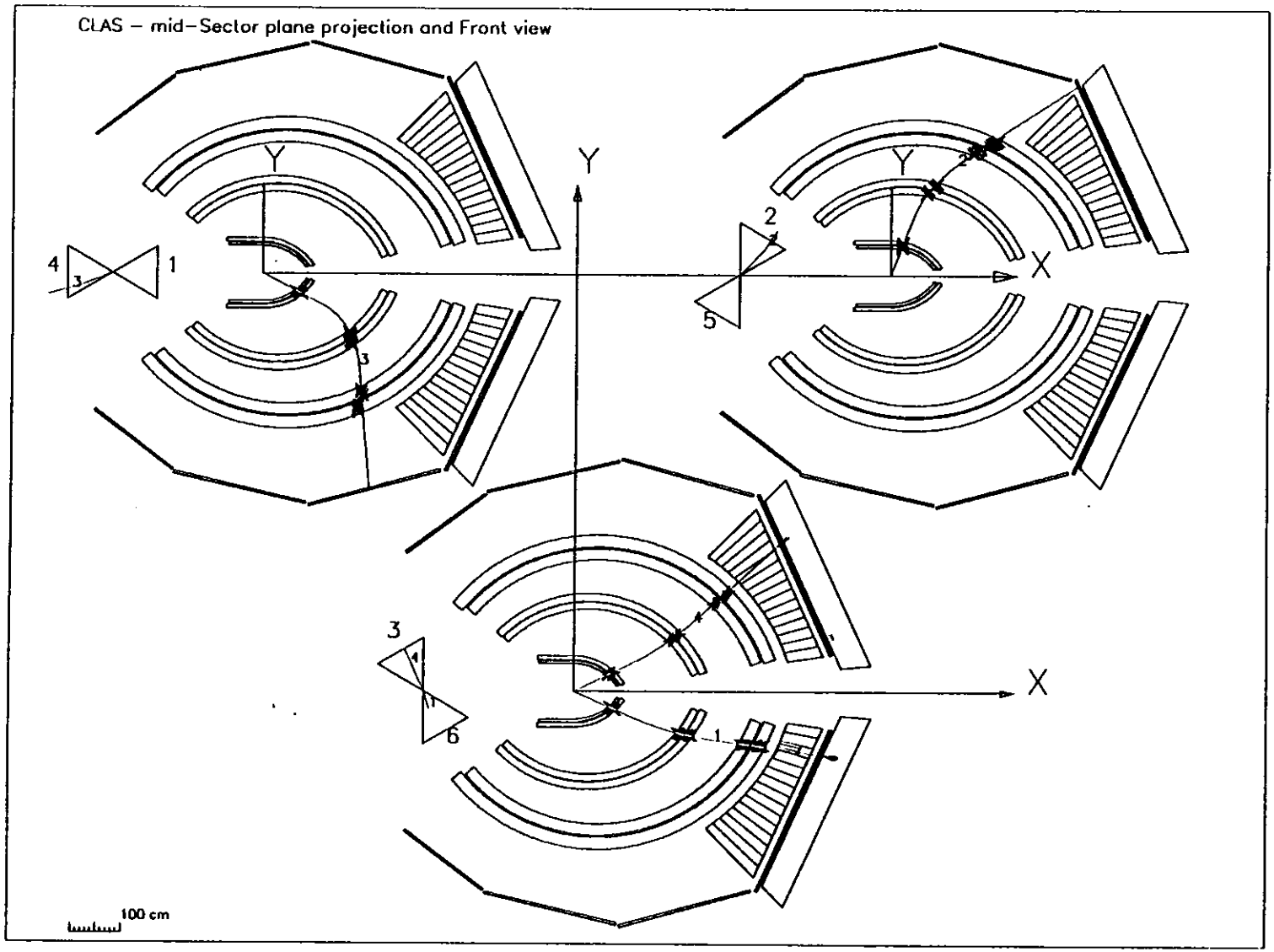

Figure 15: *Single $ep \rightarrow ep\pi^+\pi^-$ event as seen in CLAS; $E = 4$ GeV, $W = 1.7$ GeV, $Q^2 = 1$ GeV^2.*

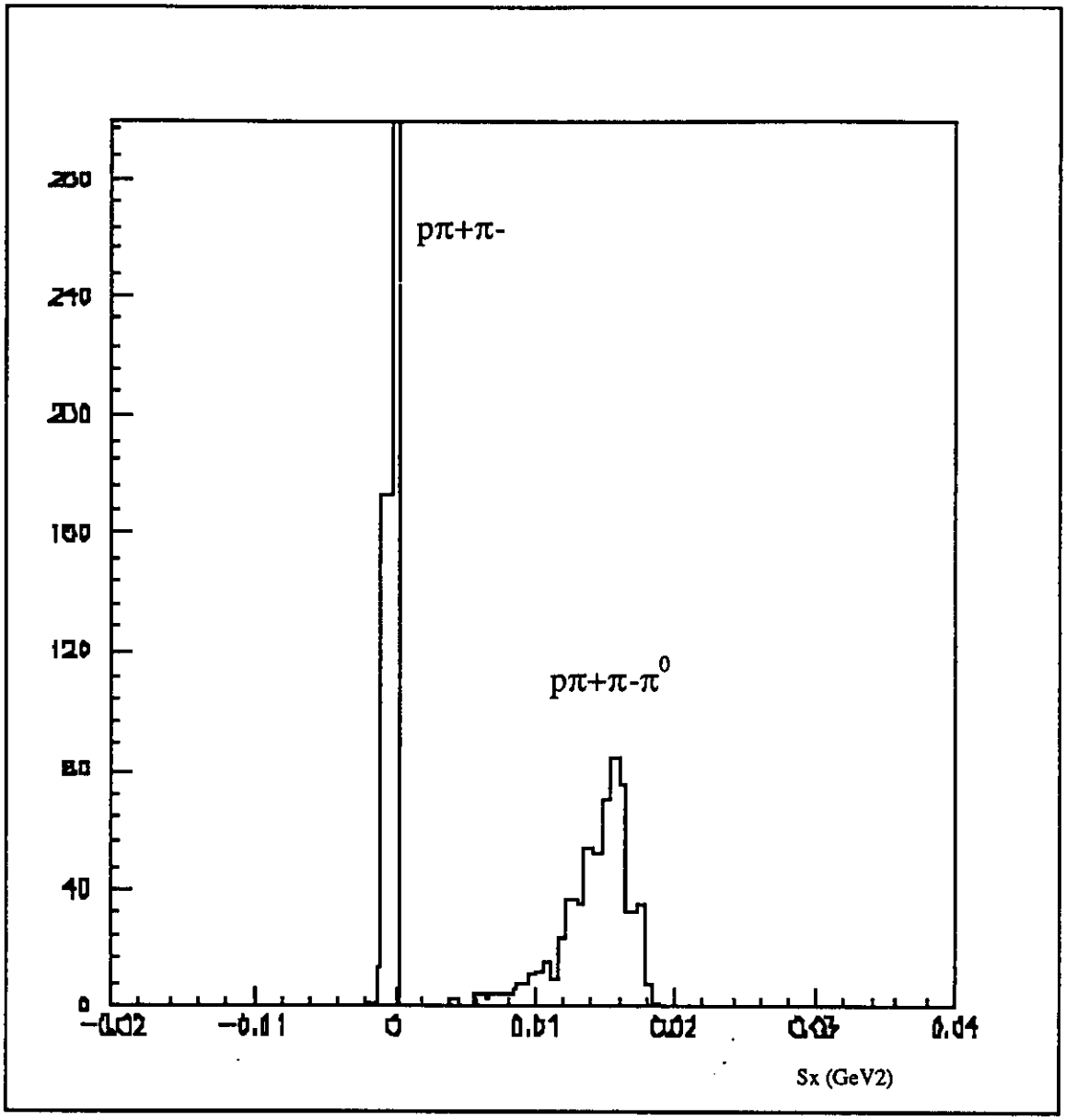

Figure 16: Missing mass spectrum for $ep \rightarrow ep\pi^+\pi^- +$ X, if $p\pi^+\pi^-$ are detected in CLAS .

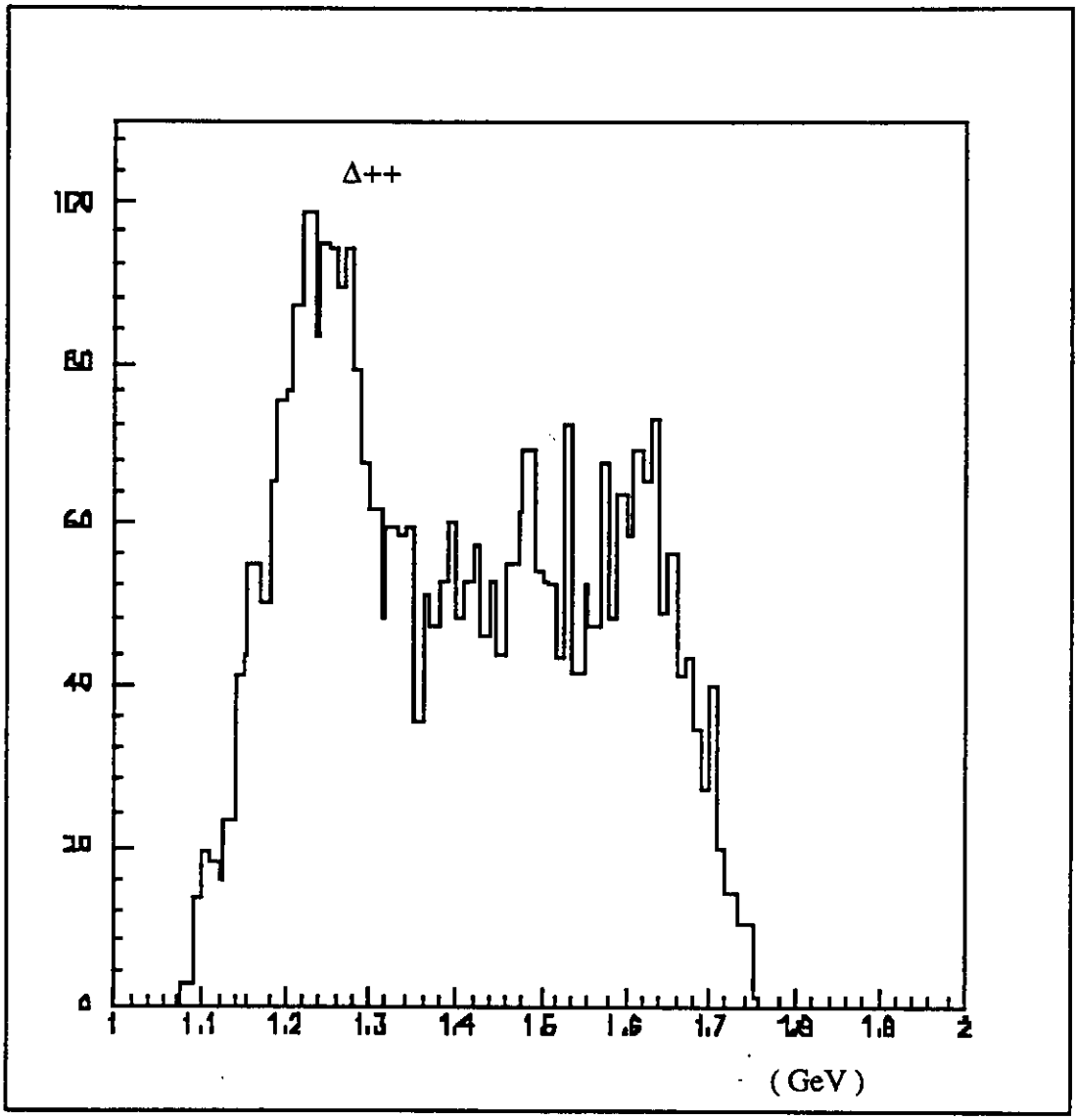

Figure 17: *Invariant mass spectrum of the $p\pi^+$ pair if $(p\pi^+\pi^-)$ are detected in CLAS.*

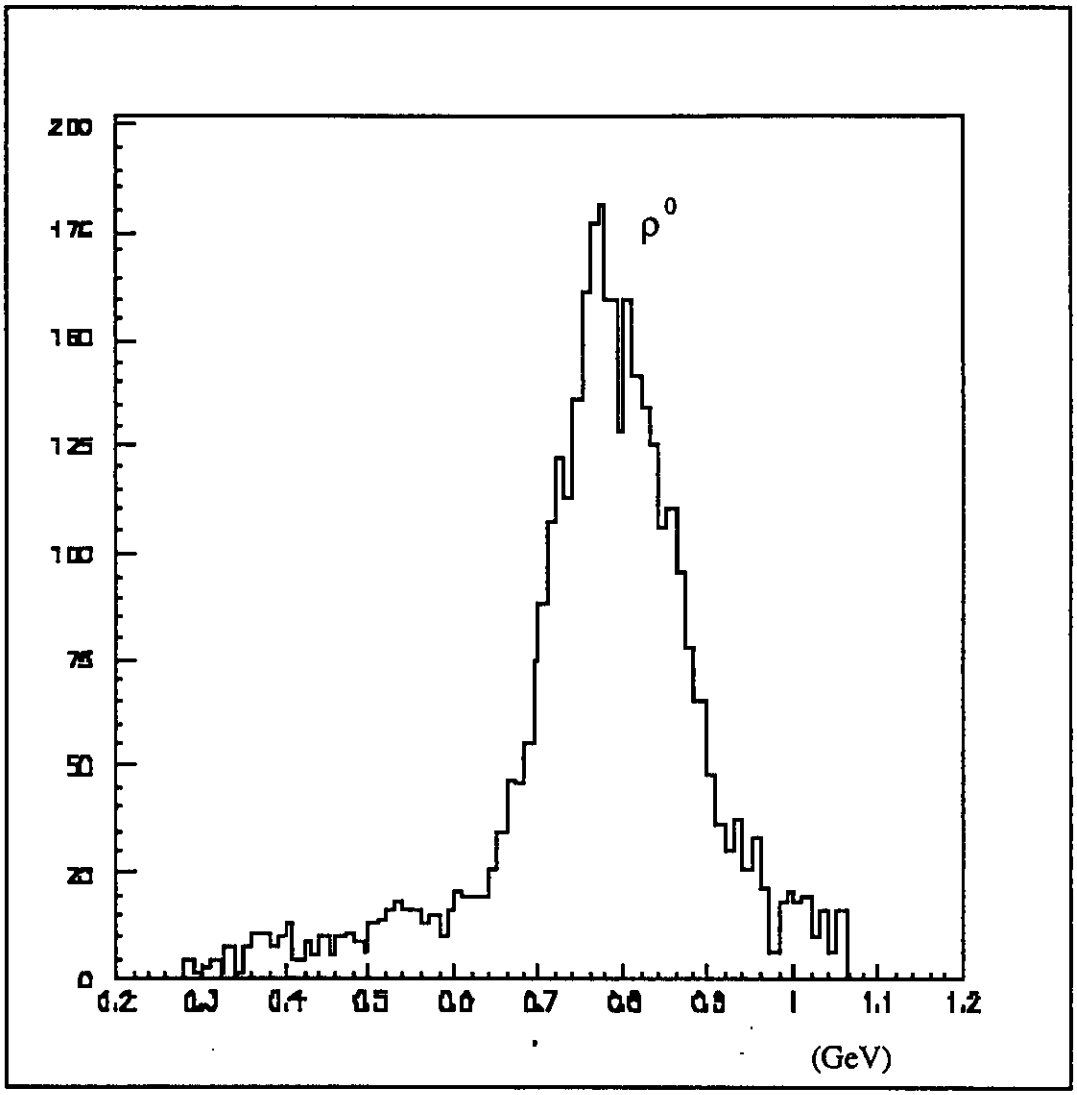

Figure 18: *Invariant mass spectrum of the $\pi^+\pi-$ pair if $(p\pi^+\pi^-)$ are detected in CLAS.*

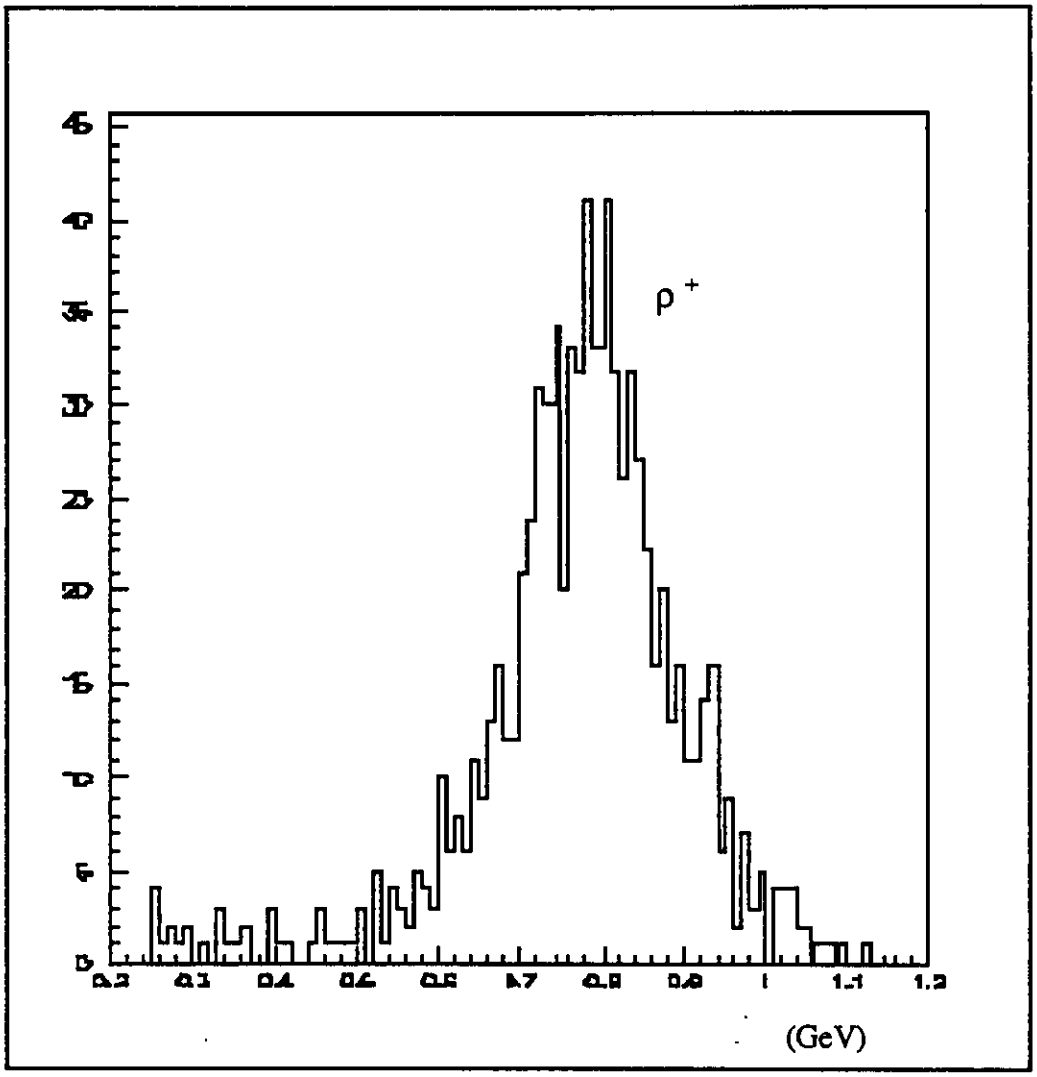

Figure 19: *Invariant mass spectrum of the $\pi^+\pi^-$ pair if $(n\pi^+\pi^0)$ or $(n\pi^+\gamma)$ are detected in CLAS.*

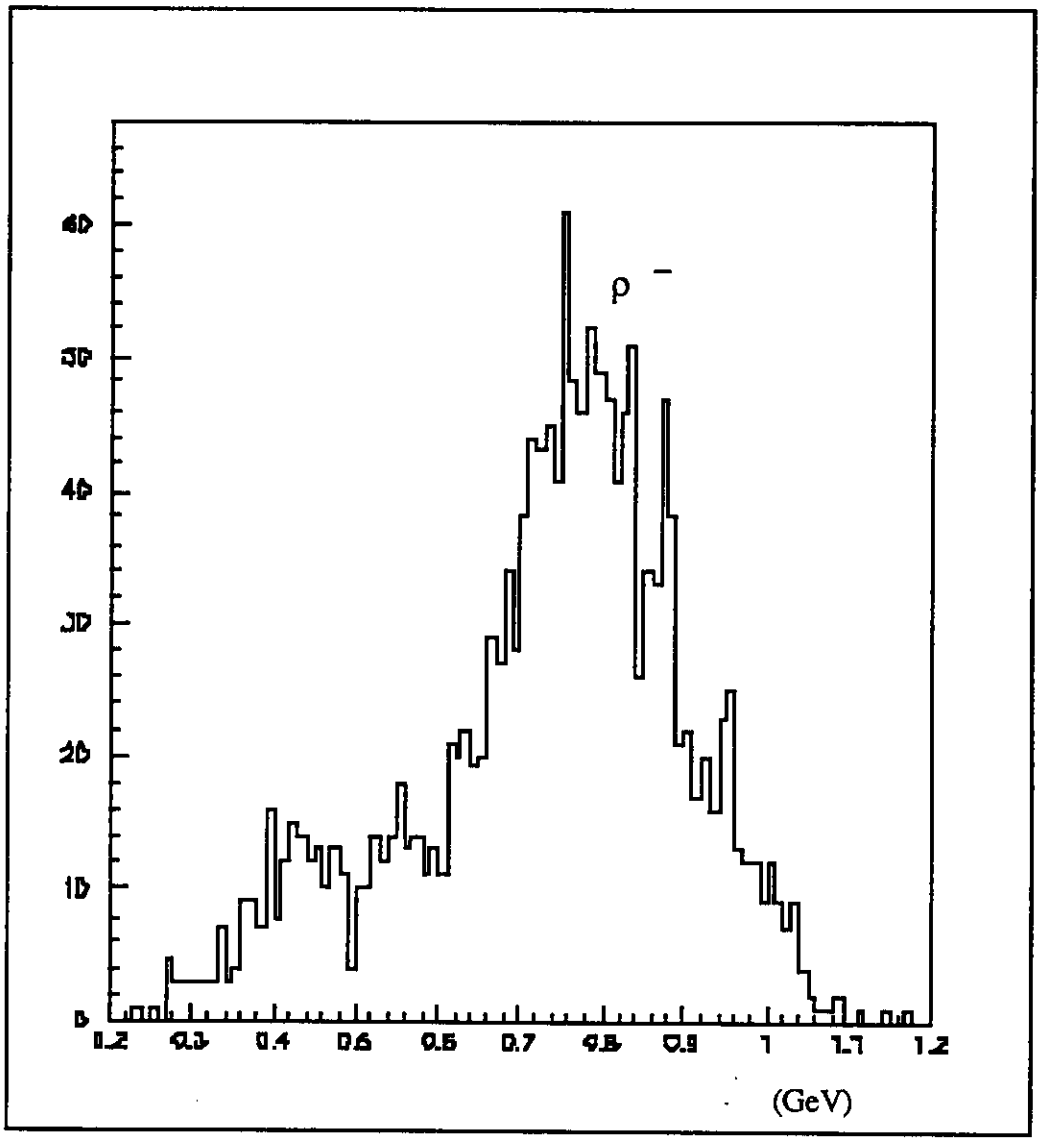

Figure 20: *Invariant mass spectrum of the $\pi^-\pi^0$ pair if $(p\pi^-\pi^0)$ or $(p\pi^-\gamma)$ are detected in CLAS (simulation on neutron target).*

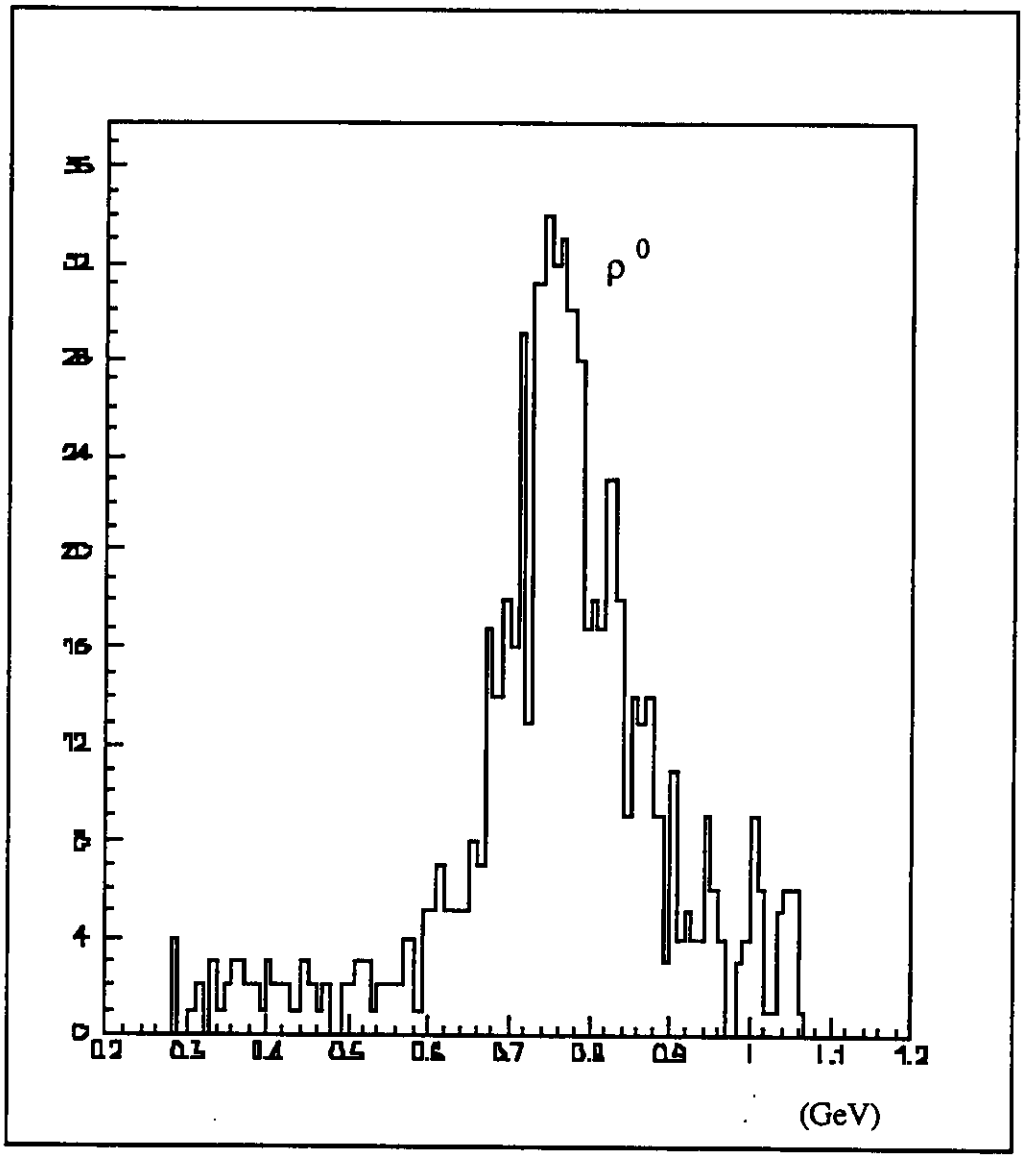

Figure 21: *Invariant mass spectrum of the $\pi^+\pi^-$ pair for $p\pi^+\pi^-$ at $t < -0.5GeV^2$.*

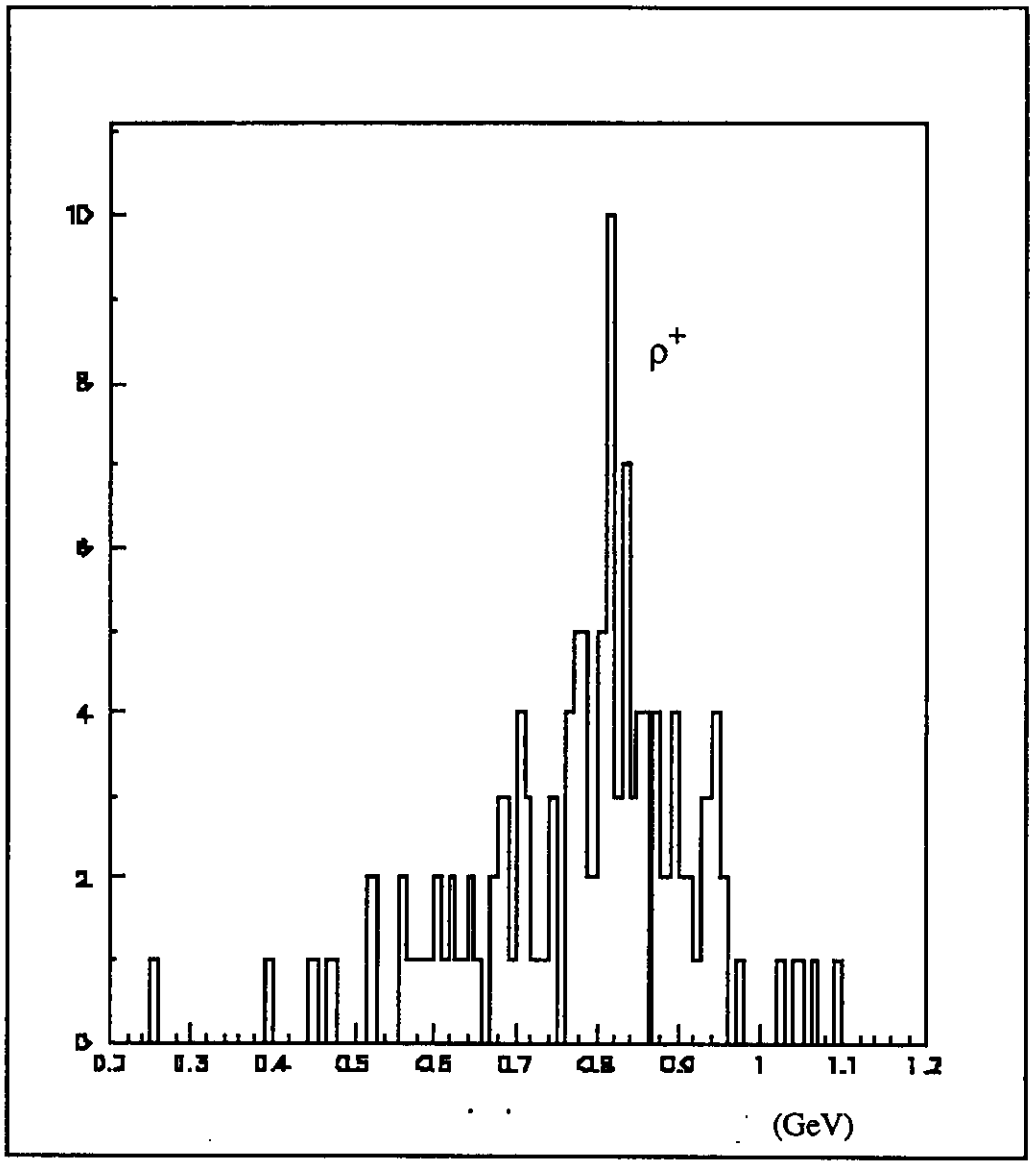

Figure 22: *Invariant mass spectrum of the $\pi^+\pi^0$ pair for $(n\pi^+\pi^0)$ at $t < -0.5GeV^2$.*

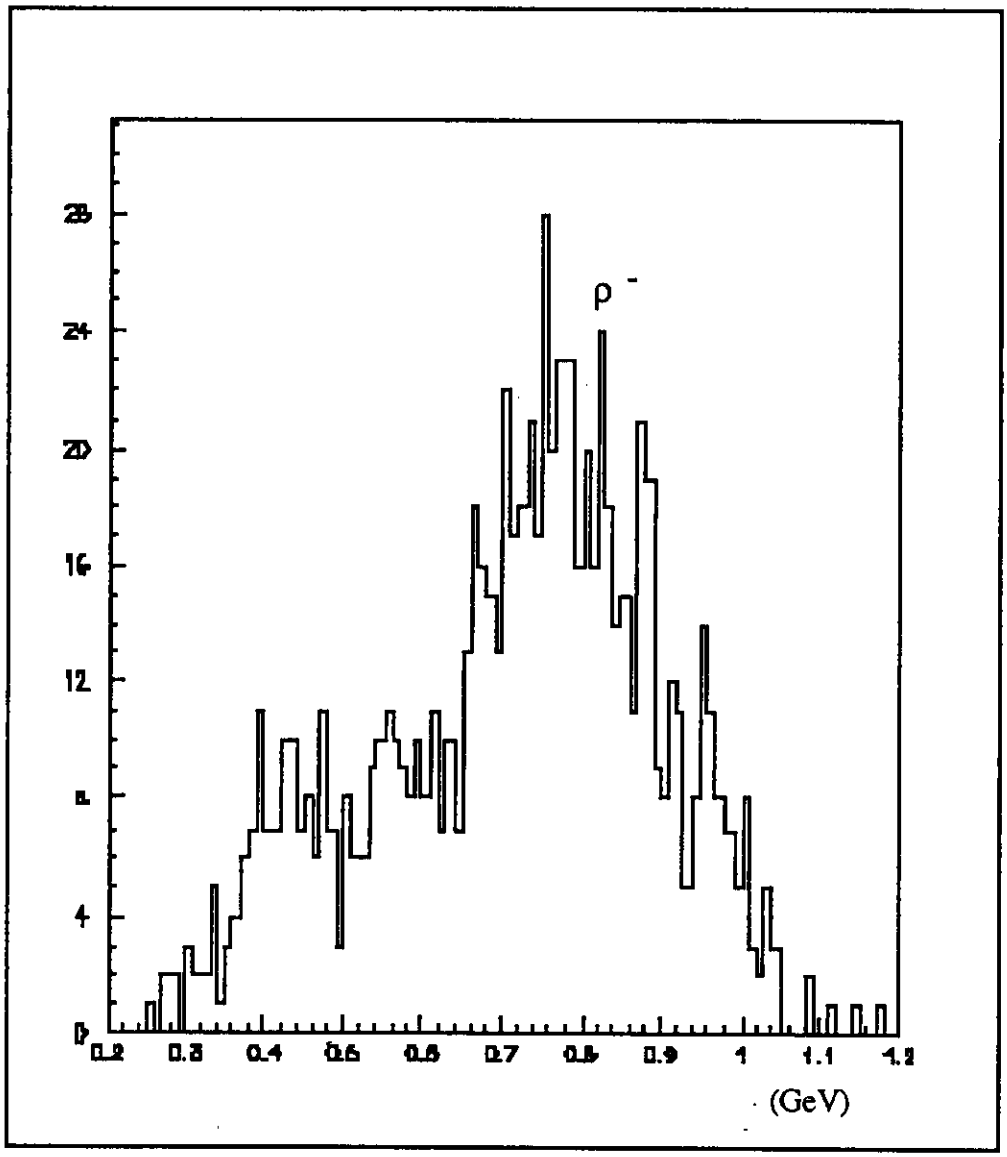

Figure 23: *Invariant mass spectrum of the $\pi^-\pi^0$ pair for $(p\pi^-\pi^0)$ at $t < -0.5GeV^2$, on neutron target.*

Detecting $n\pi^+\pi^o$ in coincidence with the electron the efficiency is about 2-3%; in this case one can add events with detection of only one photon from the neutral pion, achieving an efficiency around 7-8%. Figure 19 shows the $\pi^+\pi^o$ invariant mass reconstructed using this enlarged set of event; the ρ^+ peak is shows up quite prominently.

The same can be done for the $p\pi^-\pi^o$ channel on the neutron with an efficiency close to 10%. Figure 20 shows the $\pi^-\pi^o$ invariant mass reconstruction with a clear ρ^- production peak.

For the $\Delta^+\pi^o$ and the $\Delta^o\pi^o$ channels on proton and neutron respectively, the contribution with respect to the combinatorial background is less clear, however, in a high statistics measurement it should be possible to analyse this process, which has the advantage of comprising nearly only resonance contributions.

We have also simulated the experimental situation at high momentum transfer $t = (p' - p)^2$ or $t = (n' - n)^2$, where p, n, p',n' represent the target nucleon momenta and the outgoing nucleon momenta, respectively. As discussed above, the measurement at high t allows better separation of resonant and non-resonant contributions. The results of the simulation are shown in Figure 21 - 23.

The following table summarizes the experimental feasibility:

measurement	**information and feasibility**
$\Delta^{++}\pi^-$	mass reconstruction easy large cross section, isolation of resonances requires the analysis of angular and energy dependence
ρ^o	mass reconstruction feasible large cross section, resonances are clearly seen at backward CMS angles
$\Delta^+\pi^o$	mass reconstruction difficult due to combinatorial background but very clean to see resonances
ρ^+	mass reconstruction feasible clean observation of resonances

	especially at backward CMS angles
$\Delta^o\pi^o$	mass reconstruction difficult due to combinatorial background but very clean observation of resonances
ρ^-	mass reconstruction feasible clean separation of resonances especially at backward CMS angles

F. Count Rate Estimates

Using the calculations mentioned above and the simulations of the CLAS detector response, the statistical errors have been evaluated with the following assumptions:

Electron beam energy: E = 4 GeV

Luminosity: L = 10^{34}cm^{-2}sec^{-1}

Beam time: 500 hrs

Scattered electron energy bin: 50 MeV

Scattered electron angular bin: 2^0

π or ρ meson ϕ bin: 10^0

At $Q^2 = 0.5GeV^2$, this corresponds to a 50 MeV bin in W, and a 0.14 GeV^2 bin in Q^2. At $Q^2 = 1.0GeV^2$, this corresponds to a 90 MeV W bin, and a 0.18GeV^2 bin in Q^2.

In order to illustrate the sensitivity of the experiment to resonance contributions, we have chosen one of the predicted "missing" states, the $F_{15}(1955)$. The measurements will generate a wealth of data which will be used to also search for other resonances by analysing the angular distributions in terms of their partial wave content, and by studying the energy dependence of the respective partial waves. In Figures 24-27 the expected counts are displayed with their statistical error for the angular distributions of the various channels, with and without resonance contribution.

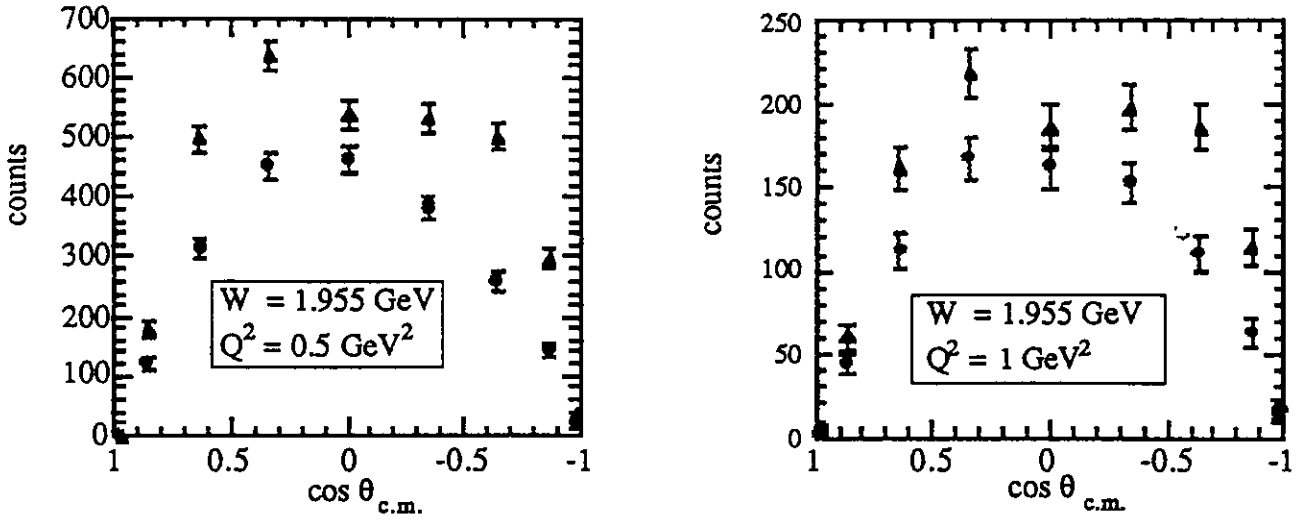

Figure 24: *Expected total counts for the π^- angular distribution in the $\Delta^+ + \pi^-$ production process. The full circles are the expected counts without the $F_{15}(1955)$ resonance; the triangles give the expected counts including the resonance.*

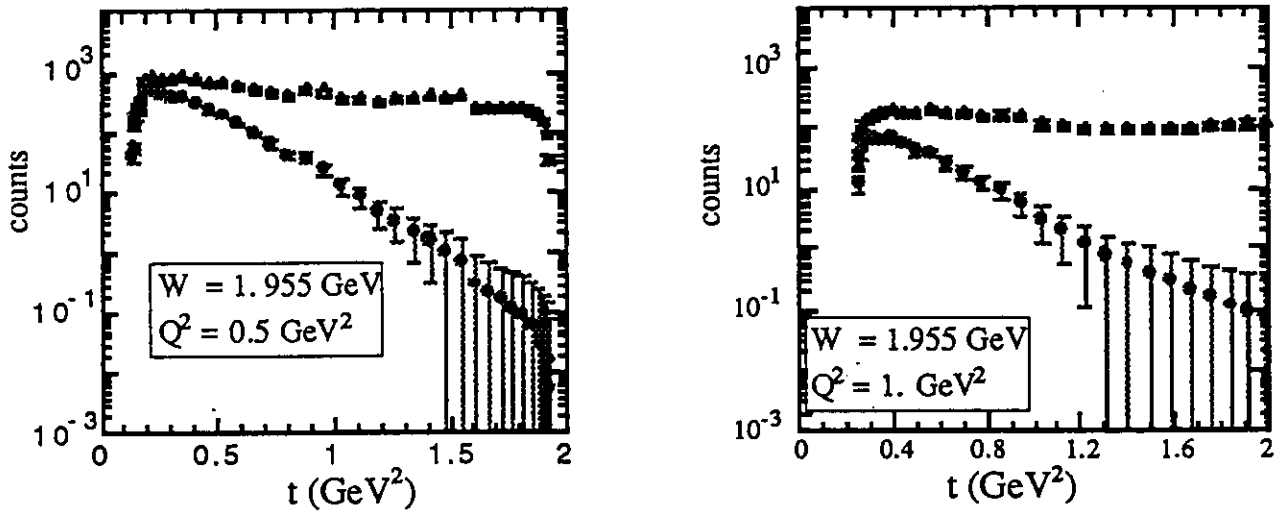

Figure 25: *Expected total counts for the ρ^0 angular distribution in the $p\rho^0$ production process. The full circles are the expected counts without the $F_{15}(1955)$ resonance; the triangles give the expected counts including the resonance.*

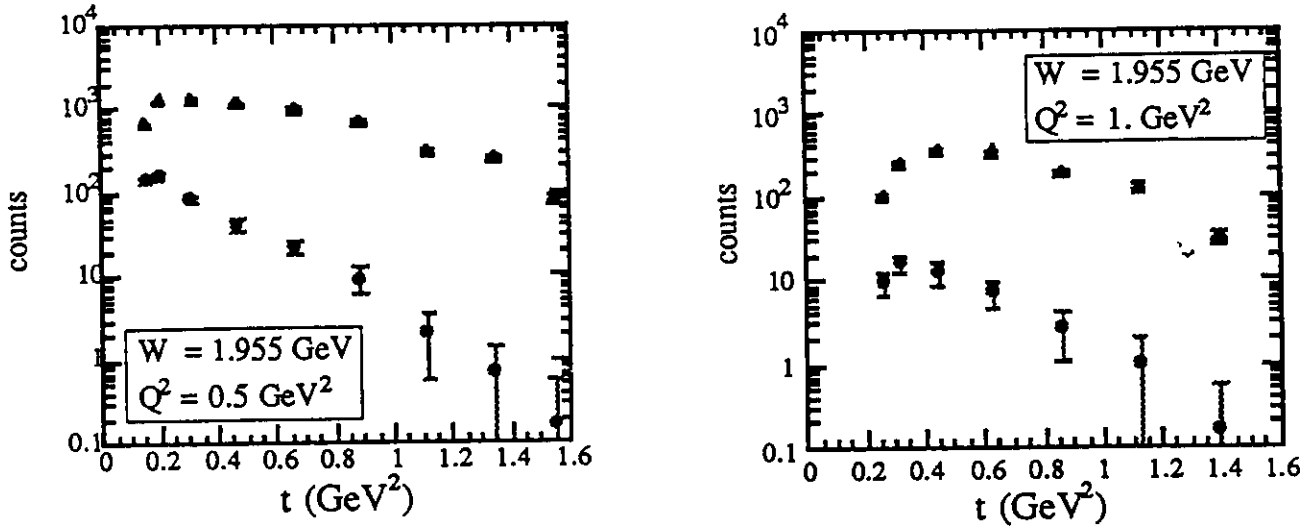

Figure 26: *Expected total counts for the ρ^+ angular distribution in the $n\rho^+$ production process. The full circles are the expected counts without the $F_{15}(1955)$ resonance; the triangles give the expected counts including the resonance.*

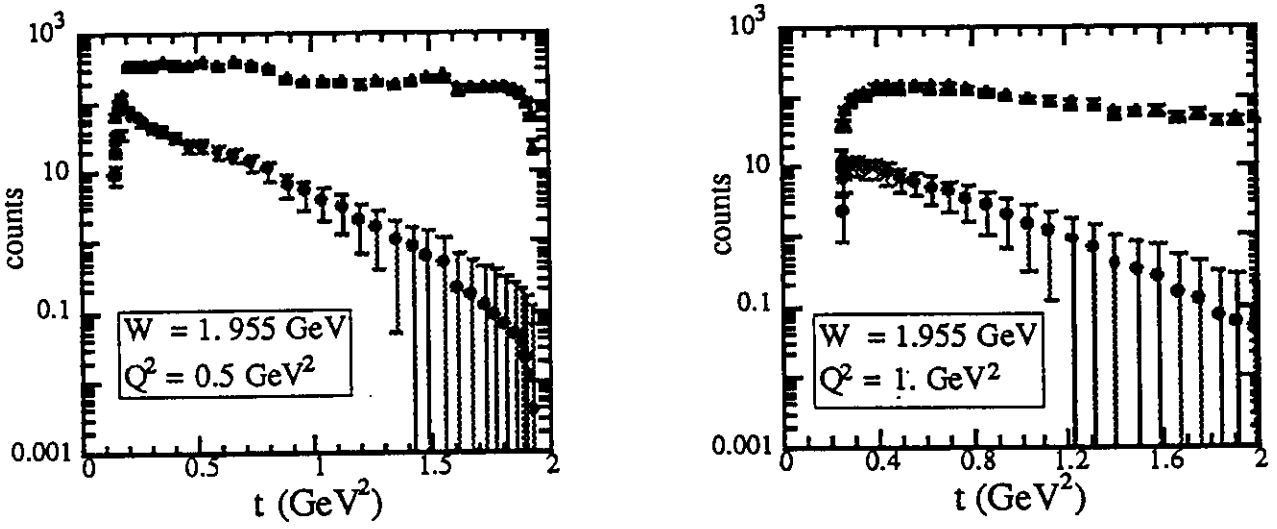

Figure 27: *Expected total counts for the ρ^- angular distribution in the $p\rho^-$ production on neutrons. The full circles are the expected counts without the $F_{15}(1955)$ resonance; the triangles give the expected counts including the resonance.*

To give a clearer idea of the sensitivity of the experiment, we summarize in table 3 the results relative to the total integrated counts, corresponding to the total cross section. For example, in the case of $\Delta^{++}\pi^-$ production we expect Born term contributions of 80,000 counts in 500hrs of beam time at W = 1.955 GeV and $Q^2 = 0.5 GeV^2$. This means a 3σ statistical error of 1%, allowing the detection of a 50nb resonant signal. In other words, the sensitivity is about 200nb per day running time. The total number of counts resulting from a $1\mu b$ resonant signal alone are reported in table 4.

Table 3: *Expected counts and sensitivities*

Process	Momentum transfer Q^2	Expected total counts in 500 hours (no resonance)	3σ statistical error	Recognizable resonance signal above 3σ	Recognizable resonance signal per day of measurement
$\Delta^{++}\pi^-$	0.5 GeV^2	80,000	1 %	50 nb	200 nb
$\Delta^{++}\pi^-$	1 GeV^2	30,000	2 %	60 nb	200 nb
$\rho^0 p$	0.5 GeV^2	140,000	0.8 %	60 nb	300 nb
$\rho^0 p$	1 GeV^2	22,000	2 %	80 nb	400 nb
$\rho^+ n$	0.5 GeV^2	17,000	2 %	100 nb	400 nb
$\rho^+ n$	1 GeV^2	1,800	7 %	30 nb	100 nb
$\rho^- p$	0.5 GeV^2	21,000	2 %	100 nb	500 nb
$\rho^- p$	1 GeV^2	4,000	5 %	50 nb	200 nb

Table 4: *Sensitivity to "missing" resonances*

Process	Expected total counts in 500 hours ($1\mu b$ resonance)	Expected total counts per day of measurement ($1\mu b$ resonance)
$\Delta^{++}\pi^-$ $\rho^0 p$	16,000	800
$\rho^+ n$	9,000	400
$\rho^- p$	13,000	600

G. Control of Systematic Errors

The proposed measurements do not require control of systematic errors that exceed the requirements of the already approved N^* proposals[17]. Therefore we describe only briefly some of the important features of CLAS that allow efficient control of many systematic effects in the measurements.

The CLAS detector offers a number of ways to control systematic uncertainties which are due to the large acceptance of this detector and are not available in multiple arm magnetic spectrometer experiments.

(1) The full kinematics will be measured at one fixed setting, therefore eliminating uncertainties related to time dependent factor, like beam energy, charge integration, beam position , etc.

(2) Elastic $ep \rightarrow ep$ scattering will be measured simultaneously with the normal data taking. Since the elastic cross section is known at the few percent level this process allows a precise calibration of the acceptance.

(3) The inclusive inelastic electron flux will be measured simultaneously allowing to establish the absolute cross section. This will also allow a precise check of the detector uniformity.

(4) The missing mass distribution in reactions such as $p(e,e'p)\pi^0$, $p(e,e'p)\eta$, $p(e,e'\pi^+)n$, and $p(e,e'p\pi^+)\pi^-$ can be used to check angle and momentum reconstruction for charged tracks, measure the detection efficiency for photons, π^0, η, and neutrons.

(5) Measurement of the full ϕ distribution in single $N\pi$ and $\Delta\pi$ production rather than only a few ϕ points, allows an excellent control of the uniformity of the detector response. The general form of the single particle production cross section is given by:

$$d\sigma/d\Omega = A + B\cos\phi + C\cos(2\phi),$$

where A, B, C are independent of ϕ (ϕ being the azimuthal angle of the $\pi\Delta$ or $p\rho$ production plane with respect to the electron scattering plane). Such a parametrization must give a perfect fit to the measured cross section. Any systematic deviation from such a behaviour would indicate systematic uncertainties in the determination of the detector acceptance.

The combination of these checks will allow an excellent control of systematic errors with an accuracy much below the required level.

H. Run Time Request

The running conditions of this experiment are identical to the conditions of some of the experiments proposed by the N* collaboration. A total of 500 hours

of beam time (to be split between 2 and 4 GeV, and hydrogen and deuterium targets) has been approved for all N* collaboration experiments. Part of the run time of this experiment can therefore be concurrent with this first beam time package. However, due to the lower efficiency for the detection of multi-hadron events and due to the lower efficiency for the detection of neutrals, we request an additional beam time of 500 hours at 4 GeV with magnetic field at one half of its maximum value, to be split between hydrogen and deuterium targets.

I. Trigger and Beamline Instrumentation

The proposed measurement will use the same inclusive electron trigger, high pressure hydrogen and deuterium gas targets, a charge integrating Faraday cup, and other equipment as the already approved experiments of the N^* program. The expected inclusive electron trigger rate is less than 1000 $\sec^{-1}$. In case the CLAS trigger level 2 is operational at the time of the measurement, a trigger requiring an additional charged hadron could be used to reduce background triggers.

K. Summary

The proposed experiment will provide accurate information about the Q^2 dependence of the $\Delta\pi$ and $N\rho$ production cross sections. Resonance excitation of several poorly studied resonances will be studied, and their electromagnetic transition formfactors will be determined by employing partial wave analysis techniques. The two-pion reaction channels are particularly sensitive to some of the "missing" states with masses around 2 GeV/c^2. The proposed measurement will generate very significant amount of information about these states. Using an electron beam allows variation of Q^2 which will facilitate the search for these states. The proposed measurements are complementary to other approved experiments (like the ω electroproduction measurement[16]). In addition to analysing the angular and energy dependence of the $\Delta\pi$ and $N\rho$ channels, we will also investigate the Δ and ρ decay distributions which are sensitive to resonance contributions as well.

Using the CEBAF Large Acceptance Spectrometer CLAS, charged and neutral particles in the final state can be detected with reasonable efficiency.

References:

1. A.J.G. Hey and J. Weyers, Phys. Lett. 48B, 69 (1974);
   W.N. Cottingham and I.H. Dunbar, Z. Phys. C2, 41 (1979)
2. N. Isgur and G. Karl, Phys. Rev. D23, 817 (1981);
   R. Koniuk and N. Isgur, Phys. Rev. D21, 1868 (1980);
   M.M. Giannini, Rep. Prog. Phys. 54, 453 (1990)
3. D.M. Manley, CEBAF internal report (not published)
4. Cambridge Bubble Chamber Group, Phys. Rev. 155, 1477 (1967);
   ABBHHM Collaboration, Phys. Rev.175, 1669 (1968);
   Lüke and Söding - Springer Tracts in Mod. Phys. 59 (1971)
5. A. Piazza et al., Lettere al nuovo cimento ,12, 403 (1970)
6. P. Joos et al., Phys. Lett., 52B, 481 (1974);
   V. Eckart et al., Nucl. Phys. B55, 45 (1973);
   K. Wacker et al., Nucl. Phys. B144, 269 (1978)
7. P. Stichel and M. Scholz, Nuovo Cimento 34, 1381 (1964)
8. M. Locher and W. Sandhas, Z.f. Physik 195, 461 (1966)
9. H.M. Pilkuhn, Relativistic Particle Physics, Springer Verlag (1979), 164
10. H.J. Weber and H. Arenhövel, Phys. Rep. 36, 277 (1978)
11. S.M. Berman and S. Drell, Phys.Rev.133, 3B, B791 (1964)
    P. Söding, Phys. Lett. 19, 702(1966)
12. H.H. Bingham et al., Phys. Rev. Lett.24, 955 (1970)
13. V. Burkert, Proceedings of the Bad Honnef Workshop, 1984, Springer Tracts in Mod. Phys. 234 (1984)
    V. Burkert, Int. J. Mod. Phys. E, Vol.1, 421 (1992)
14. F. Foster and G. Hughes, Z. Phys. C14, 123 (1982)
    V. Burkert and Zhujun Li, private communication
    P. Corvisiero, L. Mazzashi, M. Ripani, private communication
16. CEBAF Proposal PR-91-024
17. CEBAF Proposals PR-89-037,-038,-039,-040,-042,-043
18. K. F. Liu and C. W. Wong, Phys. Rev. D28, 170 (1983)